

Interference Mitigation with a Modified ASKAP Phased Array Feed on the 64 m Parkes Radio Telescope

A.P. Chippendale*

G. Hellbourg[†]

Abstract — We present results from a first attempt to mitigate radio frequency interference in real-time during astronomical measurements with a phased array feed on the 64 m Parkes radio telescope. Suppression of up to 20 dB was achieved despite errors in estimating the interference spatial signature. Best results were achieved in the clean excision of a narrowband and stationary clock signal that originates from the receiver’s digital back-end system. We also contribute a method to interpolate valid beamformer weights at interference-affected channels. Correct initial beam weights are required to avoid suppressing the desired signal.

1 AN ASKAP PAF AT PARKES

A phased array feed (PAF) is a dense array of antenna elements at the focus of a concentrator that, with digital beamforming, can produce multiple simultaneous antenna beams of high sensitivity throughout a wide field of view. We trialled interference mitigation with a Mk. II PAF system [1] built by CSIRO for the Australian Square Kilometre Array Pathfinder (ASKAP) telescope and modified by CSIRO and the Max Planck Institute for Radio Astronomy (MPIfR) for deployment on the Effelsberg 100 m telescope. Our experiments took place during a scientific commissioning phase on the 64 m Parkes telescope [2].

The ASKAP PAF [1] is a connected-element “chequerboard” array [3] operating over 0.7–1.8 GHz. Modifications for MPIfR involved the addition of selective filters to reject broad-band radio frequency interference (RFI) [2]. The experiment described here has however used an unmodified ASKAP filter covering 0.7–1.2 GHz.

The digital beamformer can simultaneously form 36 dual-polarisation beams, each of 384 MHz bandwidth, from the PAF’s 188 antenna elements. The beamformer also calculates array covariance matrices (ACMs) with 1 MHz resolution and integrated fine filter bank (FFB) spectra of the beamformer outputs with 18.5 kHz resolution.

Parkes has more challenging RFI than the radio-quiet site that the ASKAP PAF was designed for

*CSIRO Astronomy and Space Science, PO Box 76, Epping, 1710, Australia, e-mail: Aaron.Chippendale@csiro.au

[†]Department of Astronomy, University of California, 339 Campbell Hall, Berkeley, CA 94710, USA

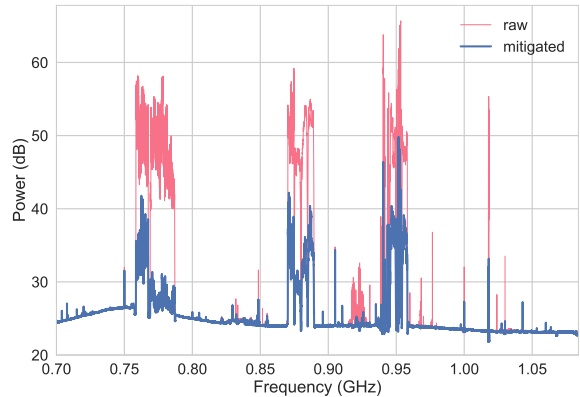


Figure 1: Median spectrum at Parkes with and without mitigation applied to a boresight maxSNR beam.

[4]. Figure 1 shows median beamformed spectra, with and without mitigation, for maximum signal-to-noise ratio (maxSNR [5]) weights over a 13 min observation with 18.5 kHz resolution. Table 1 lists dominant signals in this data. RFI scans over the 0.7–1.8 GHz range of the PAF, before beamforming, are given in [2]. The broader RFI status at Parkes is summarised on the observatory’s website¹.

2 SPATIAL MITIGATION WITH PAFS

Blind spatial filtering is proposed to perform RFI mitigation. The implemented approach involves (1) estimating the interfering signal subspace from the ACM, and (2) updating the beamformer weights to create spatial nulls towards the RFI. The viability of this technique has been demonstrated via simulation for full ASKAP [6] and by an experiment on ASKAP’s six-antenna Boolardy Engineering Test Array (BETA) [7]. This experiment successfully imaged a celestial source in a 1 MHz channel that was otherwise saturated by interference from GPS L2 over 200 times stronger than the desired signal.

Here we trial spatial filtering across the full 384 MHz system bandwidth and evaluate its impact on 18.5 kHz resolution spectra. We explore the efficacy of the technique on a wider variety of

¹http://www.parkes.atnf.csiro.au/observing/NEW/RFIstatus_June2016.pdf

Table 1: Dominant RFI Identification

Frequency (MHz)	Bandwidth	Service	n_{opt}	Comment	Label
773.000	30 MHz	4G mobile telecom	> 10	Tower transmitters (FDD-LTE)	A
880.000	20 kHz	4G mobile telecom	> 10	Tower transmitters	B
947.500	12.5 MHz	2/3/4G mobile telecom	> 10	Tower transmitters (LTE/GSM)	C
976.593	<18.5 kHz	Clock (CSIRO)	1	Seen at 976.609 MHz	D
1018.000	500 kHz	Aeronautical radiolocation	4	Parkes VOR/DME transponder	E

RFI signals and measure its impact on spectral-line observations of a celestial source.

2.1 Experimental method at Parkes

We used FFB spectra to assess the performance of various mitigation algorithms and their parameters. Each beam was initiated with maxSNR bore-sight beam weights [8] with different real-time RFI mitigation algorithms and parameters. The first beam remained unprocessed for reference. Both orthogonal and oblique projectors with various RFI subspace dimension were trialled as in [7]. The subspace dimension is closely related to the number of RFI sources, their bandwidths, and their relative motion to the telescope [9].

ACMs were continuously downloaded to estimate the RFI subspace and compute the spatial filter, before updating beam weights. The system completes an ACM download and beam weights upload every 15 s. Eight cycles of ACM downloads and weights uploads were required to apply mitigation to the full 384 MHz bandwidth because the ACM calculation operates on 48 MHz at a time. This resulted in a 120 s update period for any given 1 MHz channel. This slow rate, together with the five-fold reduction in beam feature size for the 64 m Parkes antenna with respect to the 12 m ASKAP antennas, affects the attenuation of RFI sources moving relatively to the telescope. The update rate could, however, be increased significantly by refining software.

The user-defined *on-the-sky* ACM integration time was 0.5 s, resulting in a 2 s accumulation period as the ACM calculation in firmware uses every fourth sample. The 18.5 kHz FFB spectra were integrated for 2 s and were downloaded every 4.5 s.

The experiments ran over two 384 MHz bands centred at 891.5 MHz and 1340.5 MHz. At each band, we made measurements both with the antenna stationary and tracking a celestial source at the sidereal rate of $0.25^\circ/\text{min}$. We tracked flux calibrator PKS B0407–658 [10] and a reference position offset by $+10'$ in right ascension. Only results of the band centred at 891.5 MHz are presented as they contain more fixed terrestrial sources of RFI.

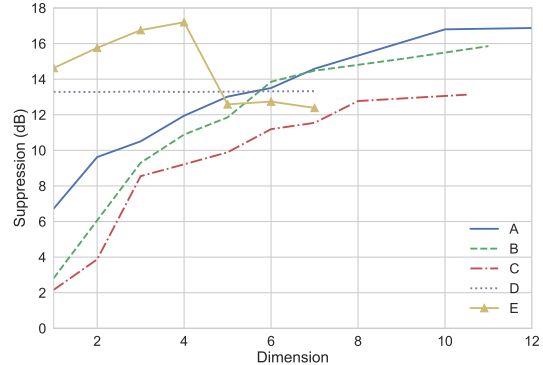


Figure 2: Median suppression achieved over 4 min by oblique projection versus RFI subspace dimension with stationary antenna. Labels match signals to Table 1.

3 RESULTS

3.1 Suppression and subspace dimension

Figure 2 shows RFI attenuation as a function of the dimension n of the projected-out RFI subspace. This plots the ratio in dB of the total power, in each signal sub-band of Table 1, between a beam with no mitigation and a beam with oblique projection mitigation. Only data from when the antenna was stationary were used. The distance measuring equipment (DME) signal (E) at 1018 MHz achieves peak suppression at $n = 4$ and the narrowband clock signal (D) does so at $n = 1$. Suppression of the mobile telecommunication base-station signals (A-C) continues to rise at $n = 10$.

Figure 3 shows the change in RFI suppression between the tracking and stationary telescope. The level of suppression is more consistent when the telescope is stationary. Error in estimating the RFI subspace also limits suppression. Performance can be improved by using reference antennas tracking RFI sources to more accurately estimate their subspace [11], reducing ACM integration time to reduce subspace smearing [9] caused by relative motion between RFI sources and the telescope, and by increasing beam weight update rates so that the mitigation is still valid when applied.

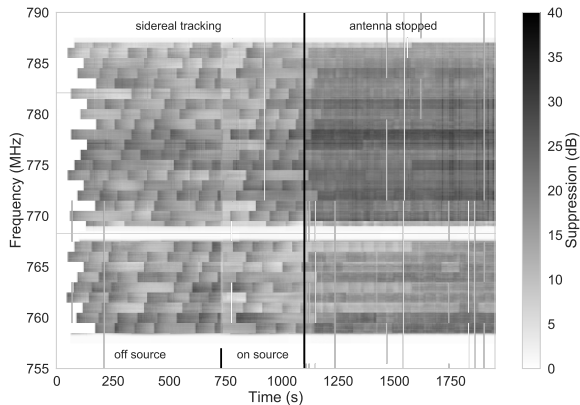


Figure 3: Suppression versus telescope motion for 4G mobile telecom (FDD-LTE) base-station signals.

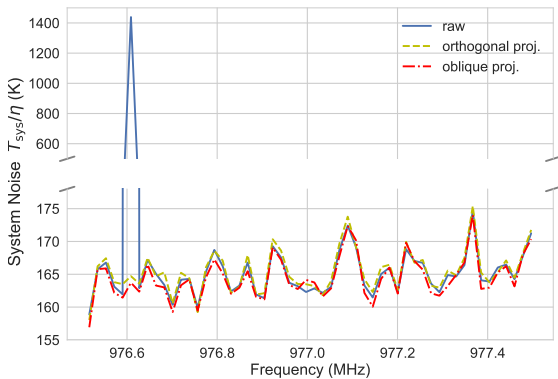


Figure 4: Clean removal of coarse filter bank read-out clock with negligible system temperature increase.

3.2 Clean excision of a narrowband signal

Expecting the current implementation to work best on stationary signals, we explored performance on a tone generated by the ASKAP digital receiver that is narrower than an 18.5 kHz FFB channel. The source is a 256 MHz FPGA clock that is multiplied by 32/27 to read out the digital receiver’s 1 MHz resolution oversampled coarse filter bank [12].

Figure 4 shows that this signal, which appears at 976.6 MHz due to direct sampling in the second Nyquist zone, is neatly mitigated to the noise floor by both orthogonal and oblique projection with $n = 1$. This plot shows the beam equivalent system-temperature-on-efficiency T_{sys}/η measured on PKS B0407–658 assuming a flux model² fit to data in the Parkes catalogue [10]. Both mitigation algorithms change system temperature by less than 1 K with respect to the unmitigated spectrum. The typical system temperature here is higher than re-

²<https://www.sao.ru/cats/cgi-bin/pkscat90.cgi>

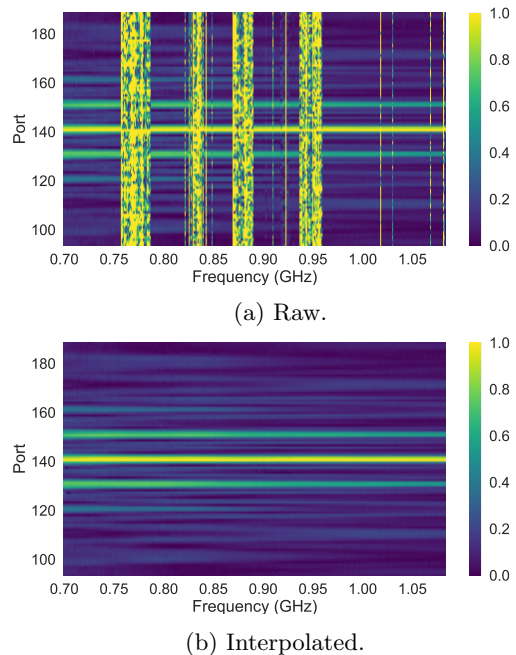


Figure 5: MaxSNR beam weight amplitudes.

ported in [2], likely because we initialised the system with 35 day-old beam weights made at different azimuth and elevation and without adjustment for changes in system status since the weights were last calibrated.

3.3 Interpolating correct initial weights

Correct initial beam weights, that maximise the desired signal, are required for algorithms that suppress RFI and retain the desired signal. Figures 5a and 6a show that the initial maxSNR beam weights are corrupted at some frequencies by RFI. Here all weights were normalised by the weights of the port with the highest typical weight amplitude³.

Figures 5b and 6b show that we can recover the weights at interference-affected channels. Amplitude is interpolated independently for each port by iteratively fitting a polynomial to its weight amplitude as a function of frequency and removing outliers that are likely to be interference-affected channels at each iteration. Before fitting a polynomial to the weight phase of a given port, we first removed a bulk linear phase (delay) estimated by taking the Fourier transform of the normalised weights with respect to frequency. We then unwrapped the phase and iteratively fit a polynomial to interference-free channels as described above. In Figure 6b, weights corrupted by RFI are replaced with an evaluation of the fitted polynomials plus the bulk linear phase.

³PAF port 141 in the numbering of ACES Memo 001 at <http://www.atnf.csiro.au/projects/askap/ACES-memos>.

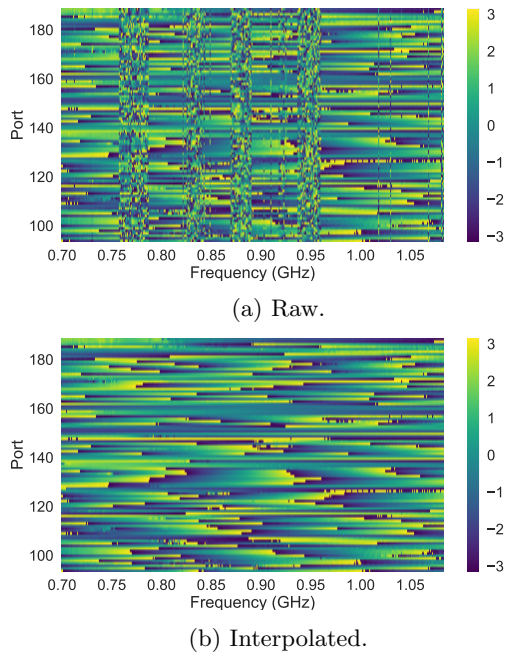


Figure 6: MaxSNR beam weight phases (radians).

4 CONCLUSION

We have suppressed RFI by up to 20 dB in real-time observations with a PAF on the Parkes telescope. Suppression could be improved by reducing the integration time and increasing the download rate of ACMs to account for dynamic RFI environments, and by correlating PAF ports against reference antennas directed at RFI sources to enhance subspace estimation. Within current limitations, best performance was achieved on a narrowband and stationary clock signal originating from the PAF backend. This was cleanly mitigated to the noise floor with no reduction in system sensitivity. Finally, we demonstrated successful interpolation of beam weights at interference-affected channels. This is immediately useful for general PAF beamforming in addition to being necessary for mitigation algorithms that robustly preserve the desired signal.

Acknowledgments

The Parkes radio telescope is part of the ATNF, which is funded by the Commonwealth of Australia for operation as a National Facility managed by the CSIRO. MPIfR financed the PAF used in this paper and its modification for a less radio-quiet site. Dr. K. Bannister and C. Haskins supported software implementation. A. Brown improved the duty cycle of the FFB integrator. Dr. B. Indermühle supported signal identification. Dr. J. Tuthill advised on the digital receiver read-out clock. Prof. L. Staveley-Smith motivated this work.

References

- [1] G. Hampson *et al.*, “ASKAP PAF ADE—advancing an L-band PAF design towards SKA,” in *2012 International Conference on Electromagnetics in Advanced Applications*, Sept 2012, pp. 807–809.
- [2] A. P. Chippendale *et al.*, “Testing a modified ASKAP Mark II phased array feed on the 64 m Parkes radio telescope,” in *2016 International Conference on Electromagnetics in Advanced Applications (ICEAA)*, Sept 2016, pp. 909–912.
- [3] S. G. Hay and J. D. O’Sullivan, “Analysis of common-mode effects in a dual-polarized planar connected-array antenna,” *Radio Science*, vol. 43, no. 6, 2008, rS6S04.
- [4] B. T. Indermühle *et al.*, “The ASKAP RFI environment as seen through BETA,” in *2016 Radio Frequency Interference (RFI)*, Oct 2016, pp. 43–48.
- [5] B. D. V. Veen and K. M. Buckley, “Beamforming: a versatile approach to spatial filtering,” *IEEE ASSP Magazine*, vol. 5, no. 2, pp. 4–24, April 1988.
- [6] R. A. Black *et al.*, “Multi-tier interference-cancelling array processing for the ASKAP radio telescope,” in *2015 IEEE Signal Processing and Signal Processing Education Workshop (SP/SPE)*, Aug 2015, pp. 261–266.
- [7] G. Hellbourg, K. Bannister, and A. Hotan, “Spatial filtering experiment with the ASKAP BETA array,” in *2016 Radio Frequency Interference (RFI)*, Oct 2016, pp. 37–42.
- [8] D. McConnell *et al.*, “The Australian Square Kilometre Array Pathfinder: Performance of the Boolardy Engineering Test Array,” *Proc. Astron. Soc. Aust.*, vol. 33, p. e042, Sep. 2016.
- [9] G. Hellbourg, “Subspace smearing and interference mitigation with array radio telescopes,” in *2015 IEEE Signal Processing and Signal Processing Education Workshop (SP/SPE)*, Aug 2015, pp. 278–282.
- [10] R. E. Otrupcek and A. E. Wright (Eds). (1990) Parkes catalogue. Australia Telescope National Facility. [Online]. Available: <https://www.parkes.atnf.csiro.au/observing/databases/pkscat90.html>
- [11] G. Hellbourg *et al.*, “Reference antenna-based subspace tracking for RFI mitigation in radio astronomy,” in *2014 IEEE Global Conference on Signal and Information Processing (GlobalSIP)*, Dec 2014, pp. 1286–1290.
- [12] J. Tuthill *et al.*, “Compensating for oversampling effects in polyphase channelizers: A radio astronomy application,” in *2015 IEEE Signal Processing and Signal Processing Education Workshop (SP/SPE)*, Aug 2015, pp. 255–260.